On velocity structure functions and the spherical vortex model for isotropic turbulence

Keri A. Aivazis
Applied Mathematics 217-50, California Institute of Technology, Pasadena, California 91125

D. I. Pullin[a)]
Graduate Aeronautical Laboratories 105-50, California Institute of Technology, Pasadena, California 91125

(Received 30 November 2000; accepted 6 March 2001)

We investigate a stochastic model for homogeneous, isotropic turbulence based on Hill's spherical vortex. This is an extension of the method of Synge and Lin [Trans. R. Soc. Can. **37**, 45 (1943)], to the calculation of higher even-order velocity structure functions. Isotropic turbulence is represented by a homogeneous distribution of eddies, each modeled by a spherical vortex. The cascade process of eddy breakdown is incorporated into the statistical model through an average over an assumed log-normal distribution of vortex radii. We calculate the statistical properties of the model, in particular order-n velocity structure functions defined by rank-n tensors for the ensemble average of a set of incremental differences in velocity components. We define $D_{i\cdots s}=\langle(u_i(\mathbf{x}+\boldsymbol{\xi})-u_i(\mathbf{x}))\cdots(u_s(\mathbf{x}+\boldsymbol{\xi})-u_s(\mathbf{x}))\rangle$, where $\langle\cdots\rangle$ denotes the ensemble average. Specifically D_{ij}, D_{ijkl}, and the longitudinal component of D_{ijklmn} are calculated directly from the spherical vortex ensemble. Matching the longitudinal components of D_{ij} and D_{ijkl} with experimental results fixes two independent model parameters. The lateral and mixed components of D_{ijkl} and the longitudinal component of D_{ijklmn} are then model predictions. © *2001 American Institute of Physics.*
[DOI: 10.1063/1.1367870]

I. INTRODUCTION

In the early 1940s, Synge and Lin[1] utilized Hill's spherical vortex as a model for homogeneous turbulence. While the spherical vortex provides a statistically tractable steady solution to Euler's equation, it lacks dissipation and an energy transfer mechanism consistent with small scale dynamics. Since the seminal work of Synge and Lin, there have been numerous investigations of vortex-based models for turbulent flows.[2–6] Townsend[2] utilized the Burgers vortex, which contains a mechanism for vortex stretching, and calculated the one-dimensional velocity spectrum for isotropic turbulence. The idea of stretched-vortex dynamics was extended by Lundgen[6] to include axisymmetric straining of vortex lines combined with an evolving, nonaxisymmetric spiral vortex structure. The stretching represents the averaged effect of larger scales while the internal spiral structure provides both a cascade mechanism and a source of energy dissipation. While the stretched-spiral vortex has been successfully applied to the calculation of the energy spectrum,[6] and some of the higher-order statistics of turbulent fine scales at small separation,[7–12] its predictive capability for larger scales is perhaps questionable.

Most quantitative vortex-based models have utilized tube and sheet-like structures remiscent of those observed in turbulent boundary layer flows. Other coherent turbulent structures include the Karman vortices observed by Roshko[13] and vorticity tubes which form in homogeneous and shear flows.[14] The source of coherent structures in homogeneous flows is unknown, if indeed such structures exist; however, large scale instability manifested in the roll-up of thin vortex layers has been suggested. Although tube-like structures can exist in a homogeneous field, they have limited appeal as a model for the statistical properties of turbulence at scales of order the integral length. In three-dimensional flows, the temporal and spatial support of tube-like structures may be moderate or small and may contribute significantly mainly to high-order velocity structure functions which are most sensitive to rare or extreme events.[15]

Presently, we consider a model for the larger structures with the purpose of building a statistical description of scales at which stretching is not a dominant dynamical mechanism. We consider homogeneous isotropic turbulence, for which all finite dimensional probablity distribution functions are invariant to rotations about the origin and mirror reflections about any plane passing through the origin. In such an idealized, isotropic, homogeneous field, the eddy would have an unbiased orientation. The spherical vortex is a natural candidate for such an eddy—symmetrical, rotational flow is secluded from potential flow by a sphere of radius a.

Synge and Lin obtained the second-order velocity correlation for turbulence consisting of an ensemble of Hill's spherical vortices, and obtained results suggesting that the spherical vortex provides a reasonable representation of a large scale turbulent eddy. Presently, we modify and extend the Synge–Lin model by incorporating cascade characteristics into the statistical model and we investigate higher-order velocity statistics. In Sec. II we define the higher-order ve-

a)Author to whom correspondence should be addressed.

locity structure functions in terms of longitudinal, transverse, and mixed components, while in Sec. III we consider the problem of the statisical representation of a turbulent field using vortex-models of eddy structure. We specialize to the Hill's spherical vortex model in Sec. IV A. Detailed calculations are given in Sec. V, where we compute the velocity structure function tensors D_{ij}, D_{ijkl}, and the longitudinal component of D_{ijklmn} for a field of locally isotropic turbulence generated by a homogeneous distribution of Hill's vortices. The model is based on an ensemble of statistically independent vortex spheres advancing with constant velocity through a fluid which is at rest at infinity. First, field averages are computed under the assumption of a single vortex type and this is followed the introduction of the Kolmogorov-type[16] log-normal distribution function governing vortex radius, which embodies the cascade process of eddy breakdown. The model contains two parameters which are fixed by matching model predictions to experimental measurements[17] of the second and fourth-order longitudinal velocity structure functions. This then allows prediction of the fourth-order lateral and mixed structure function and the sixth-order longitudinal structure function.

II. VELOCITY STRUCTURE FUNCTIONS FOR ISOTROPIC TURBULENCE

We begin by defining the velocity structure function tensors of orders 2, 3, and 4. The first order structure function is defined by the mean which is taken to be zero. The second order isotropic structure function is given by

$$D_{ij}(\xi)=\langle(u_i(\mathbf{x}+\boldsymbol{\xi})-u_i(\mathbf{x}))(u_j(\mathbf{x}+\boldsymbol{\xi})-u_j(\mathbf{x}))\rangle. \quad (2.1)$$

On writing $\tilde{u}_i=u_i(\mathbf{x}+\boldsymbol{\xi})$ and $u_i=u_i(\mathbf{x})$, the second to fourth-order even velocity structure functions are

$$D_{ij}(\boldsymbol{\xi})=\langle(\tilde{u}_i-u_i)(\tilde{u}_j-u_j)\rangle, \quad (2.2)$$

$$D_{ijk}(\boldsymbol{\xi})=\langle(\tilde{u}_i-u_i)(\tilde{u}_j-u_j)(\tilde{u}_k-u_k)\rangle, \quad (2.3)$$

$$D_{ijkl}(\boldsymbol{\xi})=\langle(\tilde{u}_i-u_i)(\tilde{u}_j-u_j)(\tilde{u}_k-u_k)(\tilde{u}_l-u_l)\rangle. \quad (2.4)$$

Orders higher than four are constructed similarly. The longitudinal structure function of order p refers to incremental differences in velocity components resolved along the vector of separation. We denote such components by u_ξ. The lateral structure function of order p refers to velocity components normal to the separation vector, denoted by either u_γ or u_λ. The mixed structure function depends on both longitudinal and lateral components, u_ξ and u_γ (or u_λ). The pth-order longitudinal and lateral structure functions are defined, respectively, by

$$D_{\underbrace{\xi\xi\cdots\xi}_{p}}=\langle(\tilde{u}_\xi-u_\xi)^p\rangle, \quad (2.5)$$

$$D_{\underbrace{\gamma\gamma\cdots\gamma}_{p}}=\langle(\tilde{u}_\gamma-u_\gamma)^p\rangle. \quad (2.6)$$

It can be shown that for an isotropic vector field $\mathbf{u}(\mathbf{x})$, the general structure functions depend on the magnitude of the separation vector and can be expressed in terms of components of the separation vector and scalar functions.[18] For the second, third, and fourth order tensors, we have

$$D_{ij}(\xi)=[D_{\xi\xi}(\xi)-D_{\gamma\gamma}(\xi)]\frac{\xi_i\xi_j}{\xi^2}+D_{\gamma\gamma}(\xi)\delta_{ij}, \quad (2.7)$$

$$D_{ijk}(\xi)=[D_{\xi\xi\xi}(\xi)-3D_{\xi\gamma\gamma}(\xi)]\frac{\xi_i\xi_j\xi_k}{\xi^3}+D_{\xi\gamma\gamma}(\xi)\left[\frac{\xi_i}{\xi}\delta_{jk}+\frac{\xi_j}{\xi}\delta_{ik}+\frac{\xi_k}{\xi}\delta_{ij}\right], \quad (2.8)$$

$$D_{ijkl}(\xi)=[D_{\xi\xi\xi\xi}(\xi)-6D_{\xi\xi\gamma\gamma}(\xi)+D_{\gamma\gamma\gamma\gamma}(\xi)]\frac{\xi_i\xi_j\xi_k\xi_l}{\xi^4}+\left[D_{\xi\xi\gamma\gamma}(\xi)-\frac{1}{3}D_{\gamma\gamma\gamma\gamma}(\xi)\right]\left[\frac{\xi_i\xi_j}{\xi^2}\delta_{kl}+\frac{\xi_i\xi_k}{\xi^2}\delta_{jl}+\frac{\xi_i\xi_l}{\xi^2}\delta_{jk}+\frac{\xi_j\xi_k}{\xi^2}\delta_{il}+\frac{\xi_j\xi_l}{\xi^2}\delta_{ik}+\frac{\xi_k\xi_l}{\xi^2}\delta_{ij}\right]+\tfrac{1}{3}D_{\gamma\gamma\gamma\gamma}(\xi)[\delta_{ij}\delta_{kl}+\delta_{ik}\delta_{jl}+\delta_{il}\delta_{jk}]. \quad (2.9)$$

In principle, analogous results can be derived for higher order tensors, but their utility diminishes due to the increase in complexity.

III. STATISTICAL REPRESENTATION OF A TURBULENT FIELD

We imagine a fluid stirred up into a state of turbulence represented by a locally isotropic, homogeneous distribution of Hill's vortices. To compute two-point correlations we first focus attention on a fixed region in space, and consider a number of separate observations of vortex distributions. Upon superimposing all such observations, we obtain an ensemble in which the frequency distribution for the field variables tends to a continuous limit.

We make several assumptions. First, we assume that fluctuations in the number of vortices in the region under consideration are statistically insignificant. Second, because the velocity field of the spherical vortex is zero at infinity in a fixed reference frame, we treat the region as infinite in extent. Since we are imposing homogeneity, the ratio of the number of vortices to the volume of our region remains finite. Therefore we pass to the limit, $V\to\infty$, $N\to\infty$ such that $N/V=n$ remains finite.

We label each vortex $1,\ldots,N$. In a given observation, the kth vortex is characterized by seven quantities, x_1^k, x_2^k, x_3^k, θ^k, ϕ^k, U^k, and a^k, three coordinates fixing its position, two coordinates fixing its orientation, and two coordinates fixing its type, giving $7N$ different quantities for each observation. Let $\boldsymbol{\alpha}_k$ be the seven-dimensional vector for vortex k. We denote by $\boldsymbol{\Phi}(\boldsymbol{\alpha}_1,\boldsymbol{\alpha}_2,\ldots,\boldsymbol{\alpha}_N)$, the continuous distribution of the $\boldsymbol{\alpha}_k$. The ensemble average of any field property B is then given by

$$\langle B\rangle=\int\cdots\int B\boldsymbol{\Phi}d\boldsymbol{\alpha}_1\cdots d\boldsymbol{\alpha}_N. \quad (3.1)$$

We assume the N vortices are stochastically independent, so that

$$\mathbf{\Phi}(\boldsymbol{\alpha}_1 \cdots \boldsymbol{\alpha}_N) = \mathbf{\Psi}^{(1)}(\boldsymbol{\alpha}_1) \cdots \mathbf{\Psi}^{(N)}(\boldsymbol{\alpha}_N). \tag{3.2}$$

Removing any dependence on the initial numbering of vortices requires

$$\mathbf{\Psi}^{(1)} = \mathbf{\Psi}^{(2)} = \cdots = \mathbf{\Psi}^{(N)}. \tag{3.3}$$

Assuming zero correlation between orientation, position and type, $\mathbf{\Psi}^{(k)}$ can be written as

$$\mathbf{\Psi}^{(k)}(\boldsymbol{\alpha}_k) = \zeta(U_k, a_k)\mu(l_k^m)\sigma(\mathbf{x}_\mathbf{k}), \tag{3.4}$$

where $\zeta(U,a)$ is the frequency distribution in type, $\mu(l^m)$ the distribution in orientation, and $\sigma(\mathbf{x})$ the distribution in position. These normalization conditions are that

$$\int \mu(l)d\Omega, \quad \int \zeta(U,a)dUda, \quad \int \sigma(\mathbf{x})dx_1dx_2dx_3,$$

are all unity. Isotropy and homogeneity give $\mu(l) = (4\pi)^{-1}$ and $\sigma(\mathbf{x}) = V^{-1}$. A distribution function for vortex type will be chosen to reflect the fractal nature of the cascade process and will be discussed later.

Velocity field statistics. The mean velocity, or first one point moment is

$$\langle \mathbf{u}(\mathbf{x}) \rangle = \int \mathbf{u}P(\mathbf{u})d\mathbf{u}. \tag{3.5}$$

We work in a frame of reference in which $\langle \mathbf{u}(\mathbf{x}) \rangle = 0$. For a vortex model based on a distribution of statistically independent vortices we denote by $\mathbf{U}(\mathbf{x}+\boldsymbol{\xi})$ and $\mathbf{U}(\mathbf{x})$, the velocities induced by the N vortices at positions $\mathbf{x}+\boldsymbol{\xi}$ and $\mathbf{x}$, respectively. Lower and upper-case symbols distinguish the field quantity induced by the set of N vortices and the field quantity induced by a single vortex. Each vortex makes an additive contribution to the velocity at the two points. Let $\tilde{u}_i(\boldsymbol{\alpha}_k)$ refer to the ith velocity component at position $\mathbf{x}+\boldsymbol{\xi}$ and $u_i(\boldsymbol{\alpha}_k)$ denote the ith velocity component at position $\mathbf{x}$, both due to vortex k. Summing over the N vortices, we have

$$U_i(\mathbf{x}+\boldsymbol{\xi}) = \sum_{k=1}^{N} \tilde{u}_i(\boldsymbol{\alpha}_k), \tag{3.6}$$

$$U_i(\mathbf{x}) = \sum_{k=1}^{N} u_i(\boldsymbol{\alpha}_k). \tag{3.7}$$

Using (3.1), the pth order structure function tensor based for a field on N noninteracting vortices is then

$$\underbrace{D_{i\cdots s}}_{p} = \int \cdots \int \mathbf{\Psi}^{(1)}(\boldsymbol{\alpha}_1) \cdots \mathbf{\Psi}^{(N)}(\boldsymbol{\alpha}_N) \sum_{k=1}^{N} (\tilde{u}_i(\boldsymbol{\alpha}_k)_k) - u_i(\boldsymbol{\alpha}_k)) \cdots \sum_{k=1}^{N} (\tilde{u}_s(\boldsymbol{\alpha}_k) - u_s(\boldsymbol{\alpha}_k)) d\boldsymbol{\alpha}_1 \cdots d\boldsymbol{\alpha}_N. \tag{3.8}$$

IV. HILL'S SPHERICAL VORTEX

A. Velocity and vorticity field

Hill's[19] spherical vortex gives a steady rotational solution to Euler's equation for an incompressible, inviscid fluid. In cylindrical polar coordinates (R,ϕ,z), if the vortex of radius a moves with speed U along the z-axis, and the location of its center is Z, then the vorticity distribution, $\boldsymbol{\omega} = (0,\omega_\phi,0)$ is

$$\omega_\phi = \begin{cases} A\,R, & R^2 + (z-Z)^2 < a^2, \\ 0, & R^2 + (z-Z)^2 > a^2, \end{cases} \tag{4.1}$$

where $A = 15\,U/2\,a^2$. The velocity field is

$$v_R = \begin{cases} 3UR\dfrac{(z-Z)}{2\,a^2}, & r \leqslant a \\ 3a^3UR\dfrac{(z-Z)}{2\,r^5}, & r \geqslant a \end{cases}, \tag{4.2}$$

$$v_z = \begin{cases} U\dfrac{5a^2 - 3(z-Z)^2 - 6R^2}{2a^2}, & r \leqslant a \\ a^3U\dfrac{3(z-Z)^2 - r^2}{2r^5}, & r \geqslant a \end{cases}, \tag{4.3}$$

where $r^2 = R^2 + (z-Z)^2$. Coordinates θ and r are defined by

$$R = r\sin\theta, \tag{4.4}$$

$$z - Z = r\cos\theta, \tag{4.5}$$

such that the component of $\mathbf{r}$ along the direction of advancement is $r\cos\theta$. Using the direction cosines l^i $(i = 1,2,3)$ defining the direction of advancement referred to an arbitrary set of axes,

$$l_1 = \sin\theta\cos\varphi, \tag{4.6}$$

$$l_2 = \sin\theta\sin\varphi, \tag{4.7}$$

$$l_3 = \cos\theta, \tag{4.8}$$

the velocity field can be recast in the following form, convenient to the calculation of averages,

$$u_i = \alpha_{ij}l^j, \quad \alpha_{ij} = \frac{3Ua^3r_ir_j}{2r^5} - \frac{Ua^3\delta_{ij}}{2r^3}, \quad r \geqslant a, \tag{4.9}$$

$$u_i = \beta_{ij}l^j, \quad \beta_{ij} = \frac{3Ur_ir_j}{2a^2} + U\left(\frac{5}{2} - \frac{3r^2}{a^2}\right)\delta_{ij}, \quad r \leqslant a. \tag{4.10}$$

From continuity, the symmetrical tensors α_{ij} and β_{ij} are divergence free with respect to either index,

$$\frac{\partial\alpha_{ij}}{\partial x_i} = \frac{\partial\alpha_{ij}}{\partial x_j} = \frac{\partial\beta_{ij}}{\partial x_i} = \frac{\partial\beta_{ij}}{\partial x_j} = 0. \tag{4.11}$$

Furthermore,

$$\alpha_{ij} = \frac{\partial\varphi_i}{\partial x_j} = \frac{\partial\varphi_j}{\partial x_i} = \alpha_{ji},$$

where

$$\varphi_i = -\frac{U\,a^3}{2\,r^3}r_i. \tag{4.12}$$

Except for derivative operators, there is an implied sum only over repeated indices at different levels.

B. Statistics for the spherical vortex ensemble

Using Hill's spherical vortex, turbulent properties can be calculated by explicit ensemble averaging. We begin by deriving the governing integrals for the velocity structure functions. A significant feature of the spherical vortex is that the velocity field is proportional to the direction cosines. This ensures that the mean is zero and greatly simplifies the average over orientation. The spatial dependence of **u** can be removed from the two-dimensional integral over the Euler angles which then reduces to averaging a rank-p tensor of direction cosines. Let $\overline{B}^{\Omega}$ denote the average of field property $B(\theta,\varphi)$ over orientation. The general expression for $\overline{B}^{\Omega}$ is given by the spherical-polar integral,

$$\overline{B}^{\Omega}=\int_0^{2\pi} d\varphi \int_0^{\pi} d\theta \sin\theta B(\theta,\varphi). \tag{4.13}$$

For B equal to a product of direction cosines, the following relations will prove useful:

$$\overline{l_i}^{\Omega}=0, \tag{4.14}$$

$$\overline{l_i l_j}^{\Omega}=\tfrac{1}{3}\delta_{ij}, \tag{4.15}$$

$$\overline{l_i l_j l_k}^{\Omega}=0, \tag{4.16}$$

$$\overline{l_i l_j l_k l_m}^{\Omega}=\tfrac{1}{15}(\delta_{ij}\delta_{km}+\delta_{ik}\delta_{jm}+\delta_{im}\delta_{jk}), \quad \text{etc.} \tag{4.17}$$

The symmetry properties of the spherical vortex ensure that all odd order correlations vanish. This contradicts experimental evidence that the third order correlation is nonzero. Nonetheless, because the spherical vortex model is a local solution to the steady Euler's equation, $(\partial_t=0,\nu=0)$, the Kármán–Howarth equation is not violated. As noted by Synge and Lin,[1] a more realistic model might include terms quadratic in the direction cosines, so that odd order correlations would not vanish in general.

The second order velocity structure function, D_{ij}, assumes a particularly simple form. Since the mean value is zero, the cross terms in the expansion of Eq. (3.8) for $p=2$ vanish leaving the sum of N identical integrals. Furthermore, isotropy ensures $D_{ii}=D_{ij}\delta_{ij}$. Hence,

$$D_{ii}=N\int \boldsymbol{\Psi}^{(k)}(\boldsymbol{\alpha}_k)(\tilde{u}_i(\boldsymbol{\alpha}_k)-u_i(\boldsymbol{\alpha}_k))^2 d\boldsymbol{\alpha}_k, \tag{4.18}$$

where $i=\xi$, γ, or λ. The script k denotes a typical vortex. For $p=4,6,8,\ldots$ cross terms of even powers remain. Referring to our preferred coordinate system, fourth order isotropic tensor of the form (2.4) can be fully specified by three independent scalar functions.[20] For the fourth-order velocity structure function, these are the longitudinal structure function $D_{\xi\xi\xi\xi}$, the lateral structure function $D_{\gamma\gamma\gamma\gamma}$, and the cross structure function $D_{\xi\xi\gamma\gamma}$, defined, respectively, by

$$D_{iiii}=\int\cdots\int \boldsymbol{\Psi}^{(1)}(\boldsymbol{\alpha}_1)\cdots\boldsymbol{\Psi}^{(N)}(\boldsymbol{\alpha}_N) \times\left[\sum_{k=1}^{N}(\tilde{u}_i(\boldsymbol{\alpha}_k)-u_i(\boldsymbol{\alpha}_k))\right]^4 d\boldsymbol{\alpha}_1\cdots d\boldsymbol{\alpha}_N, \tag{4.19}$$

with $i=\xi$ or γ, and

$$D_{\xi\xi\gamma\gamma}=\int\cdots\int \boldsymbol{\Psi}^{(1)}(\boldsymbol{\alpha}_1)\cdots\boldsymbol{\Psi}^{(N)}(\boldsymbol{\alpha}_N) \times\left[\sum_{k=1}^{N}(\tilde{u}_\xi(\boldsymbol{\alpha}_k)-u_\xi(\boldsymbol{\alpha}_k))\right]^2 \times\left[\sum_{k=1}^{N}(\tilde{u}_\gamma(\boldsymbol{\alpha}_k)-u_\gamma(\boldsymbol{\alpha}_k))\right]^2 d\boldsymbol{\alpha}_1\cdots d\boldsymbol{\alpha}_N. \tag{4.20}$$

Expanding, and appealing to isotropy and symmetry of the spherical vortex, we find

$$D_{iiii}=N\int \boldsymbol{\Psi}^{(k)}(\boldsymbol{\alpha}_k)(\tilde{u}_i(\boldsymbol{\alpha}_k)-u_i(\boldsymbol{\alpha}_k))^4 d\boldsymbol{\alpha}_k +3N(N-1)\frac{D_{ii}^2}{N^2}, \tag{4.21}$$

where $i=\xi$ or γ, and

$$D_{\xi\xi\gamma\gamma}=N\int \boldsymbol{\Psi}^{(k)}(\boldsymbol{\alpha}_k)(\tilde{u}_\xi(\boldsymbol{\alpha}_k)-u_\xi(\boldsymbol{\alpha}_k))^2 \times(\tilde{u}_\gamma(\boldsymbol{\alpha}_k)-u_\gamma(\boldsymbol{\alpha}_k))^2 d\boldsymbol{\alpha}_k+N(N-1)\frac{D_{\xi\xi}D_{\gamma\gamma}}{N^2} +2N(N-1)\frac{D_{\xi\gamma}^2}{N^2}. \tag{4.22}$$

Although isotropy ensures $D_{\xi\gamma}$ is zero, it has been retained in the above equation so that Eq. (4.22) agrees with Eq. (4.21) for the lateral component $D_{\xi\xi\xi\xi}$ upon contracting the indices, ξ and γ as required. The spherical vortex model will also be used to predict the lateral component of the sixth order structure function tensor,

$$D_{\xi\xi\xi\xi\xi\xi}=N\int \boldsymbol{\Psi}^{(k)}(\boldsymbol{\alpha}_k)(\tilde{u}_\xi(\boldsymbol{\alpha}_k)-u_\xi(\boldsymbol{\alpha}_k))^6 d\boldsymbol{\alpha}_k +15N(N-1)\frac{D_{\xi\xi}D_{\xi\xi\xi\xi}}{N^2}. \tag{4.23}$$

Since the symmetry in the Hill's spherical vortex causes the odd order structure functions to vanish, terms in the above expansions involving D_{ijk} and D_{ijklm} are zero.

V. STRUCTURE FUNCTIONS

A. Calculation of D_{ij}

The two nonzero second order structure functions $D_{\xi\xi}$ and $D_{\gamma\gamma}$ are related to the longitudinal and lateral velocity correlation functions by expanding $(\tilde{u}_i-u_i)^2$, imposing isotropy and then averaging,

$$D_{\xi\xi}(\xi)=2\langle u^2\rangle[1-f(\xi)], \tag{5.1}$$

$$D_{\gamma\gamma}(\xi)=2\langle u^2\rangle[1-g(\xi)]. \tag{5.2}$$

While the two quantities $f(\xi)$ and $g(\xi)$ are related via continuity, we will calculate them independently for the spherical vortex model and use the relationship $g=f+1/2\xi f'$ to verify the results. We now decompose the distribution function as in (3.4) and impose homogeneity and isotropy on $\mu(l_i)$ and $\sigma(x_i)$. The second order structure function is given by

$$D_{ii}=\frac{n}{4\pi}\int d\mathbf{x}\int d\mathbf{\Omega}(\tilde{u}_i-u_i)^2, \tag{5.3}$$

where the dependence of u_i and $\tilde{u}_i$ on a single vortex characterized by the vector $\boldsymbol{\alpha}_k$ is understood and where the vortex number density is $n=N/V$. We have not yet considered the distribution in type. The longitudinal structure function is given by the second moment of the increments Δu_ξ, defined by (5.3) for $i=\xi$, and the lateral structure function is given by the second moment of the increments Δu_γ, defined by (5.3) for $i=\gamma$. Next, let $\tilde{u}_i=\tilde{c}_{ij}l^j$, where

$$\tilde{c}_{ij}=\begin{cases}\tilde{\alpha}_{ij} & \tilde{r}\geqslant a\\ \tilde{\beta}_{ij} & \tilde{r}\leqslant a\end{cases} \tag{5.4}$$

and $u_i=c_{ij}l^j$, where

$$c_{ij}=\begin{cases}\alpha_{ij} & r\geqslant a\\ \beta_{ij} & r\leqslant a.\end{cases} \tag{5.5}$$

Substituting into (5.3) we find

$$D_{ii}=\frac{n}{4\pi}\int d\mathbf{x}\int d\mathbf{\Omega}[(\tilde{c}_{ij}-c_{ij})l^j]^2. \tag{5.6}$$

Let A_0 denote the point at position $\mathbf{x}$, and $\tilde{A}_0$ denote the point at position $\mathbf{x}+\boldsymbol{\xi}$. In general, two-point correlations involve moving the separation vector through all of space and allowing it to take on all orientations. This is equivalent to holding points, A_0 and $\tilde{A}_0$, fixed, and rotating a single vortex through its Euler angles, and allowing it to take on all positions in space. Upon expanding the integrand, and averaging with respect to direction, i.e., $\overline{l^il^j}=\frac{1}{3}\delta_{ij}$, the second order structure function becomes

$$D_{ii}=\frac{n}{3}\int (c_{ij}c_i^j-2c_{ij}\tilde{c}_i^j+\tilde{c}_{ij}\tilde{c}_i^j)d\mathbf{x}. \tag{5.7}$$

As the vortex is moved through space, the velocity at point A_0 is fixed by the tensor α_{ij} or β_{ij} depending on the distance between the vortex center and A_0. The same is true for the velocity at point $\tilde{A}_0$. Since the formal expressions for the velocity field are different depending on the vortex position, integrating over the volume requires partitioning the domain of integration into three regions when $\xi>2a$ and four regions when $\xi<2a$, Figs. 1 and 2.

1. Case 1: $\xi\geqslant 2a$

When the magnitude of the separation vector exceeds the vortex diameter, there are three distinct regions (see Fig. 1). In region I, both points, A_0 and $\tilde{A}_0$, are secluded from rotational flow, while in regions II and III one point is in the interior of the spherical vortex, while the other point is outside the vortex within the potential flow region. Specifically,

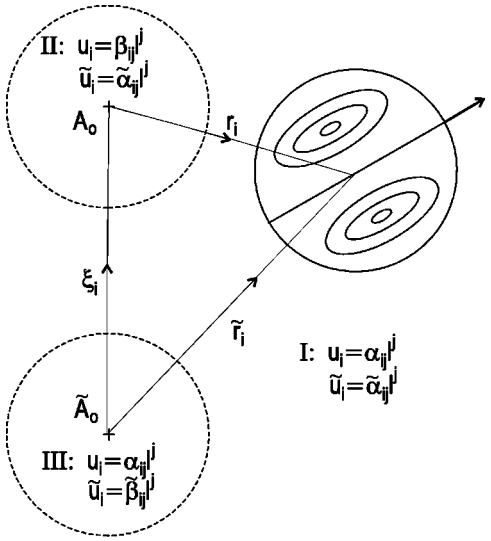

FIG. 1. Case 1: When the vortex diameter is less than the distance between points A_0 and $\tilde{A}_0$, the volume can be partitioned into three distinct regions depending on the relative position of the vortex and the two points.

$$\begin{aligned}D_{ii}(\xi)=\frac{n}{3}\Bigg\{&\int_{\mathrm{I}}(\tilde{\alpha}_{ij}\tilde{\alpha}_i^j-2\tilde{\alpha}_{ij}\alpha_i^j+\alpha_{ij}\alpha_i^j)d\mathbf{x}\\&+\int_{\mathrm{II}}(\tilde{\alpha}_{ij}\tilde{\alpha}_i^j-2\tilde{\alpha}_{ij}\beta_i^j+\beta_{ij}\beta_i^j)d\mathbf{x}\\&+\int_{\mathrm{III}}(\tilde{\beta}_{ij}\tilde{\beta}_i^j-2\tilde{\beta}_{ij}\alpha_i^j+\alpha_{ij}\alpha_i^j)d\mathbf{x}\Bigg\}.\end{aligned} \tag{5.8}$$

Using $\alpha_{ij}=\partial\varphi_i/\partial x_j$, appealing to continuity, and using Green's theorem to transform terms in (5.8) into surface integrals over Σ_{II}, Σ_{III}, and a sphere of infinite radius, this equation can be simplified. The integral on the sphere vanishes because the velocity is zero at infinity. Using that $\alpha_{ij}=\beta_{ij}$ on Σ_{II} and $\tilde{\alpha}_{ij}=\tilde{\beta}_{ij}$ on Σ_{III} allows (5.8) to be written as

$$\begin{aligned}D_{ii}(\xi)=\frac{n}{3}\Bigg\{&\int_{\Sigma_{\mathrm{II}}}(2\tilde{\alpha}_i^j\varphi_i-\alpha_i^j\varphi_i-2\beta_i^j\tilde{\varphi}_i)n_jd\sigma\\&-\int_{\Sigma_{\mathrm{III}}}\tilde{\alpha}_i^j\tilde{\varphi}_in_jd\tilde{\sigma}+\int_{\mathrm{II}}\beta_{ij}\beta_i^jd\mathbf{x}+\int_{\mathrm{III}}\tilde{\beta}_{ij}\tilde{\beta}_i^jd\mathbf{x}\Bigg\}.\end{aligned} \tag{5.9}$$

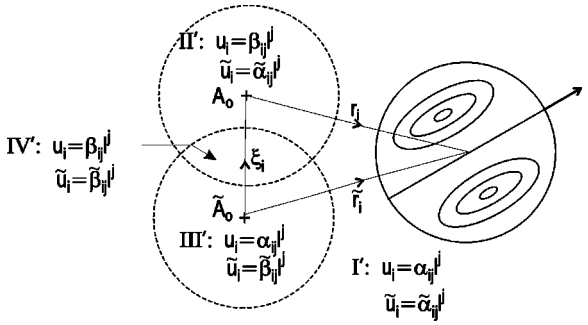

FIG. 2. Case 2: When the vortex diameter exceeds the separation distance, there is a region in which rotational flow is induced at both points A_0 and $\tilde{A}_0$. In this case there are four distinct regions to be considered.

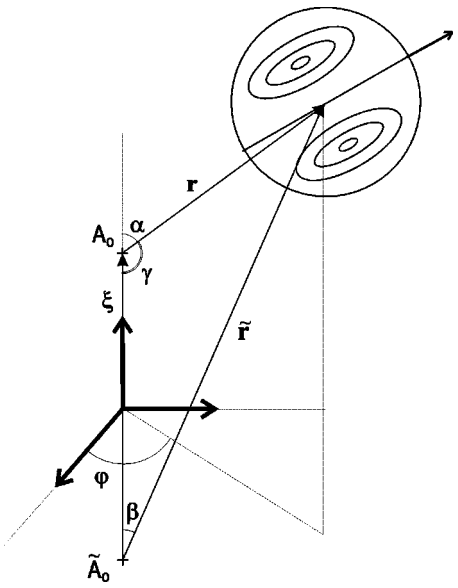

FIG. 3. The toroidal coordinate system. Each point in space is specified by $r=\|\mathbf{r}\|$, $\tilde{r}=\|\tilde{\mathbf{r}}\|$, and the polar angle φ.

The remaining integration is further simplified by changing to toroidal coordinates $(r,\tilde{r},\varphi)$, Fig. 3, in which each point P is specified by the distances, $A_0P,\tilde{A}_0P$, and the polar angle φ. Presently, the integrands are functions of r_i and $\tilde{r}_i$, and the magnitudes r and $\tilde{r}$. Let T be the transformation that takes $(\mathbf{r},\tilde{\mathbf{r}})\rightarrow(r,\tilde{r},\varphi)$,

$$T\equiv\begin{cases} r_1=r\sin\alpha\cos\varphi=f(r,\tilde{r})\cos\varphi \\ r_2=r\sin\alpha\sin\varphi=f(r,\tilde{r})\sin\varphi \\ r_3=r\cos\alpha=\dfrac{\tilde{r}^2-r^2-\xi^2}{2\xi} \\ \tilde{r}_1=\tilde{r}\sin\beta\cos\varphi=f(r,\tilde{r})\cos\varphi \\ \tilde{r}_2=\tilde{r}\sin\beta\sin\varphi=f(r,\tilde{r})\sin\varphi \\ \tilde{r}_3=\tilde{r}\cos\beta=\dfrac{\tilde{r}^2-r^2+\xi^2}{2\xi} \end{cases} \tag{5.10}$$

where

$$f(r,\tilde{r})=\left(\frac{r^2+\tilde{r}^2}{2}-\frac{(\tilde{r}^2-r^2)^2}{4\xi^2}-\frac{\xi^2}{4}\right)^{1/2}, \tag{5.11}$$

and the volume element is $dV=r\,\tilde{r}\,dr\,d\tilde{r}\,d\phi/\xi$. We define $\alpha_{ij}\overset{T}{\rightarrow}\Lambda_{ij}$, $\beta_{ij}\overset{T}{\rightarrow}\Theta_{ij}$, $\varphi_{ij}\overset{T}{\rightarrow}\Phi_{ij}$, and $n_j\overset{T}{\rightarrow}\nu_j$.

The surfaces, Σ_{II}, and Σ_{III} are now defined by surfaces of constant r, and $\tilde{r}$, respectively. By symmetry, the two volume integrals in Eq. (5.9) are equivalent. Under the coordinate transformation $D_{ii}(\xi)$ becomes (see Fig. 4),

$$\begin{aligned} D_{ii}(\xi)=\frac{n}{3}\Bigg\{ & \int_0^{2\pi}d\phi\int_{\xi-a}^{\xi+a}d\tilde{r}\frac{a\tilde{r}}{\xi}(2\tilde{\Lambda}_i^j\Phi_i-\Lambda_i^j\Phi_i \\ & -2\Theta_i^j\tilde{\Phi}_i)\nu_j-\int_0^{2\pi}d\phi\int_{\xi-a}^{\xi+a}dr\frac{ar}{\xi}\tilde{\Lambda}_i^j\tilde{\Phi}_i\tilde{\nu}_j \\ & +2\int_0^{2\pi}d\phi\int_0^{a}dr\int_{\xi-a}^{\xi+a}d\tilde{r}\frac{r\tilde{r}}{\xi}\Theta_{ij}\Theta_i^j\Bigg\}. \end{aligned} \tag{5.12}$$

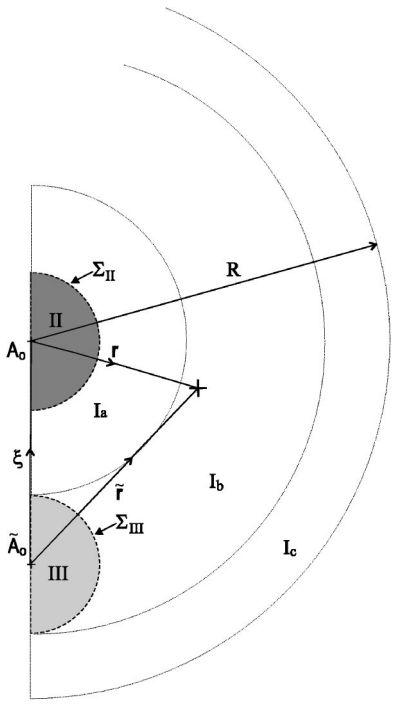

FIG. 4. Partitioning the domain of integration: Case 1.

The coordinate system has been oriented so that $\hat{e}_3$ lies along the direction of the vector ξ $(\hat{e}_3=\hat{e}_\xi)$. Therefore, $D_{\xi\xi}$ corresponds to $i=3$, and $D_{\gamma\gamma}$ corresponds to $i=2$. Upon representing the integrand in toroidal coordinates, and performing the above integration, we find

$$D_{\xi\xi}(\xi)=\frac{4}{21}na^3\pi U^2\left(10-7\left(\frac{a}{\xi}\right)^3\right)\xi\geqslant 2a, \tag{5.13}$$

$$D_{\gamma\gamma}(\xi)=\frac{2}{21}na^3\pi U^2\left(20+7\left(\frac{a}{\xi}\right)^3\right)\xi\geqslant 2a. \tag{5.14}$$

The mean-square velocity is given by

$$\langle u^2\rangle=\tfrac{1}{2}\lim_{\xi\rightarrow\infty}D_{\xi\xi}(\xi)=\tfrac{1}{2}\lim_{\xi\rightarrow\infty}D_{\gamma\gamma}(\xi)=\tfrac{20}{21}na^3\pi U^2. \tag{5.15}$$

2. Case 2: $\xi\leqslant 2a$

When the distance separating the two points is less than the vortex diameter, there is a region in space where the vortex induces rotational flow at both points. Referring to Fig. 2,

$$\begin{aligned} D_{ii}(\xi)=\frac{n}{3}\Bigg\{ & \int_{\mathrm{I}'}(\tilde{\alpha}_{ij}\tilde{\alpha}_i^j-2\tilde{\alpha}_{ij}\alpha_i^j+\alpha_{ij}\alpha_i^j)d\mathbf{x} \\ & +\int_{\mathrm{II}'}(\tilde{\alpha}_{ij}\tilde{\alpha}_i^j-2\tilde{\alpha}_{ij}\beta_i^j+\beta_{ij}\beta_i^j)d\mathbf{x} \\ & +\int_{\mathrm{III}'}(\tilde{\beta}_{ij}\tilde{\beta}_i^j-2\tilde{\beta}_{ij}\alpha_i^j+\alpha_{ij}\alpha_i^j)d\mathbf{x} \\ & +\int_{\mathrm{IV}'}(\tilde{\beta}_{ij}\tilde{\beta}_i^j-2\tilde{\beta}_{ij}\beta_i^j+\beta_{ij}\beta_i^j)d\mathbf{x}\Bigg\}. \end{aligned} \tag{5.16}$$

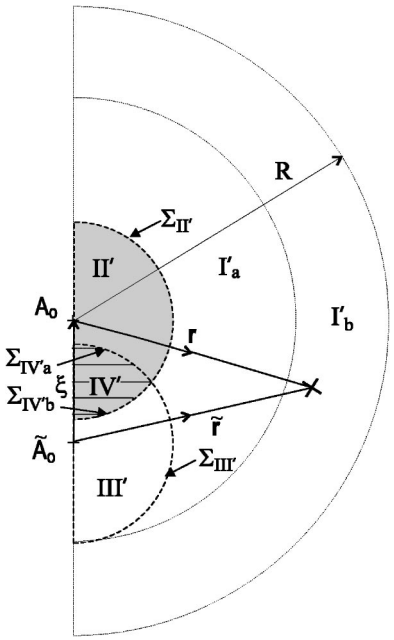

FIG. 5. Partitioning the domain of integration: Case 2.

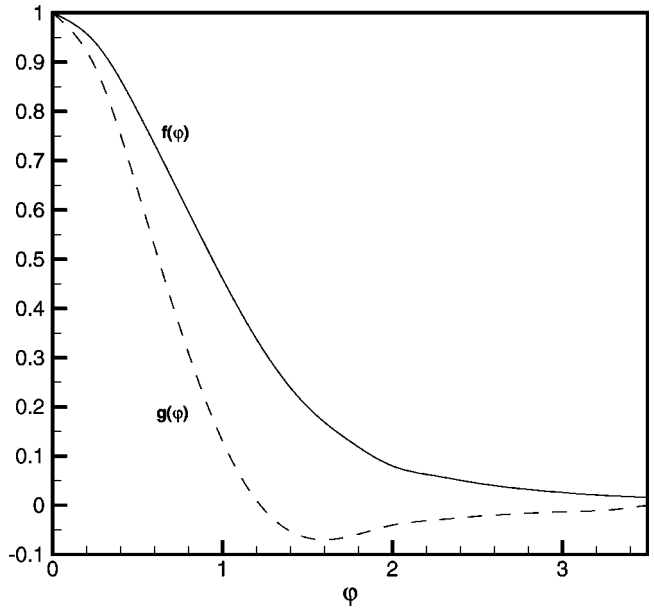

FIG. 6. Second order longitudinal and lateral correlation functions due to a single vortex type, Eqs. (5.20) and (5.21), $\varphi=\xi/a$.

Upon introducing the potential φ_i, we can invoke Green's theorem again to simplify the above integral. Appealing to symmetry arguments and using the T-transformation we obtain (see Fig. 5),

$$D_{ii}(\xi)=\frac{n}{3}\Bigg\{\int_0^{2\pi}d\varphi\int_a^{\xi+a}d\tilde{r}\frac{a\tilde{r}}{\xi}(2\tilde{\Lambda}_i^j\Phi_i-\Lambda\Phi_i-2\Theta_i^j\tilde{\Phi}_i)\nu_j-\int_0^{2\pi}d\varphi\int_a^{\xi+a}dr\frac{ar}{\xi}\tilde{\Lambda}_i^j\tilde{\Phi}_i\tilde{\nu}_j+2\int_0^{2\pi}d\phi\int_a^{\xi+a}dr\int_{\xi-r}^{a}d\tilde{r}\frac{r\tilde{r}}{\xi}\tilde{\Theta}_i^j\tilde{\Theta}_{ij}+2\int_0^{2\pi}d\varphi\int_{\xi-a}^{a}dr\int_{\xi-r}^{a}d\tilde{r}\frac{r\tilde{r}}{\xi}(\Theta_i^j\Theta_{ij}-\tilde{\Theta}_i^j\Theta_{ij})+2\int_0^{2\pi}d\varphi\int_{\xi-a}^{a}dr\frac{ar}{\xi}(2\Theta_i^j\tilde{\Phi}_i-\tilde{\Lambda}_i^j\tilde{\Phi}_i)\tilde{\nu}_j\Bigg\}. \tag{5.17}$$

Setting $i=3$, and carrying out the above integration,

$$D_{\xi\xi}(\xi)=na^3\pi U^2\left[2\left(\frac{\xi}{a}\right)^2-\frac{25}{24}\left(\frac{\xi}{a}\right)^3+\frac{5}{64}\left(\frac{\xi}{a}\right)^5-\frac{3}{896}\left(\frac{\xi}{a}\right)^7\right]\quad(\xi\leqslant 2a). \tag{5.18}$$

For the lateral function, $i=2$,

$$D_{\gamma\gamma}(\xi)=na^3\pi U^2\left[\frac{21\,504}{5376}\left(\frac{\xi}{a}\right)^2-\frac{14\,000}{5376}\left(\frac{\xi}{a}\right)^3+\frac{1470}{5376}\left(\frac{\xi}{a}\right)^5-\frac{81}{5376}\left(\frac{\xi}{a}\right)^7\right]\quad(\xi\leqslant 2a). \tag{5.19}$$

Under the assumption of local isotropy, the second order structure function is related to the longitudinal and transverse velocity correlation coefficients, $f(\xi)$ and $g(\xi)$, by Eqs. (5.1) and (5.2). Solving for $f(\xi)$ and $g(\xi)$, we obtain results consistent with Synge and Lin, Fig. 6,

$$f(\xi)=\begin{cases}\dfrac{7}{10}\left(\dfrac{a}{\xi}\right)^3 & (\xi\geqslant 2a)\\ 1-\dfrac{21}{20}\left(\dfrac{\xi}{a}\right)^2+\dfrac{35}{64}\left(\dfrac{\xi}{a}\right)^3-\dfrac{21}{512}\left(\dfrac{\xi}{a}\right)^5+\dfrac{9}{5120}\left(\dfrac{\xi}{a}\right)^7 & (\xi\leqslant 2a),\end{cases} \tag{5.20}$$

$$g(\xi)=\begin{cases}-\dfrac{7}{20}\left(\dfrac{a}{\xi}\right)^3 & (\xi\geqslant 2a)\\ 1-\dfrac{21}{10}\left(\dfrac{\xi}{a}\right)^2+\dfrac{175}{128}\left(\dfrac{\xi}{a}\right)^3-\dfrac{147}{1024}\left(\dfrac{\xi}{a}\right)^5+\dfrac{81}{10240}\left(\dfrac{\xi}{a}\right)^7 & (\xi\leqslant 2a).\end{cases} \tag{5.21}$$

We remark that the results of Synge and Lin contain a small error in their expression for $g(\xi)$, where their coefficient of $(\xi/a)^5$ omits a factor of 2. Knowledge of $f(\xi)$ enables us to compute the Taylor microscale, λ, and the macro length scale, L in terms of the vortex size a,

$$\lambda=\left[-\left(\frac{d^2f}{d\xi^2}\right)_{\xi=0}\right]^{-(1/2)}=\sqrt{\frac{10}{21}}a, \tag{5.22}$$

$$L=\int_0^\infty f(\xi)d\xi=\frac{35}{32}a. \tag{5.23}$$

Synge and Lin used the statistical model outlined here to compute the second order velocity correlation and the turbulent length scales λ and L. We depart from the Synge–Lin

statistical model and introduce an average over vortex type which is physically motivated by the fractal structure of the energy cascade.

B. Average over vortex type

Kolmogorov[16] used particle fragmentation as a model for eddy breakdown to develop the log-normal hypothesis for the energy dissipation rate, $\varepsilon(\mathbf{x},t)$. This was formalized by Yaglom[21] in a model for self-similar eddy breakdown. More recently, Bernal[22] investigated the statistics of large scale vortex structure in turbulent mixing layers, finding that the distribution of vortex circulation is also log-normal. Presently, we appeal to the Yaglom model for self-similar eddy breakdown and utilize the natural assumption of a log-normal distribution function for the vortex radii,

$$\zeta(u,\sigma)=\begin{cases}\dfrac{(2\pi)^{-1/2}}{\sigma u}\exp\left[-\dfrac{1}{2}\left(\dfrac{\log(u)}{\sigma}\right)^2\right] & (a>0)\\ 0 \quad (a\leqslant 0),\end{cases} \tag{5.24}$$

where $u=a/a_0$, a_0 is a length scale defined formally by the mean of $\log a$ and σ is a dimensionless variance. The assumption of log-normality for $\varepsilon(\mathbf{x},t)$, and consequently a, provides a natural physical representation for the distribution of scales characteristic of inertial-range transfer. This is not represented dynamically in the Hill's spherical vortex model.

Upon averaging over vortex position and vortex orientation, the second order structure function has the form,

$$D_{ii}\left(\frac{\xi}{a},na^3,U^2\right)=D_{ii,<}H\left(2-\frac{\xi}{a}\right)+D_{ii,>}H\left(\frac{\xi}{a}-2\right), \tag{5.25}$$

where H denotes the Heaviside function and $D_{ii,<}$ and $D_{ii,>}$ correspond to the second order structure functions for case 2 and case 1, respectively. Recasting D_{ii} in a more suitable form prior to averaging, we find

$$D_{ii}\left(\frac{\xi}{a_0},u,na_0^3,U^2\right)=\hat{D}_{ii,<}H\left(u-\frac{\xi}{2a_0}\right)+\hat{D}_{ii,>}H\left(\frac{\xi}{2a_0}-u\right). \tag{5.26}$$

Specifically, for the longitudinal and lateral function, we have

$$\begin{aligned}\hat{D}_{\xi\xi,<}&=\pi U^2 na_0^3\left[2\left(\frac{\xi}{a_0}\right)^2u-\frac{25}{24}\left(\frac{\xi}{a_0}\right)^3+\frac{5}{64}\left(\frac{\xi}{a_0}\right)^5u^{-2}-\frac{3}{896}\left(\frac{\xi}{a_0}\right)^7u^{-4}\right],\\ \hat{D}_{\xi\xi,>}&=\pi U^2 na_0^3\frac{4}{21}\left[10u^3-7\left(\frac{a_0}{\xi}\right)^3u^6\right],\end{aligned} \tag{5.27}$$

and

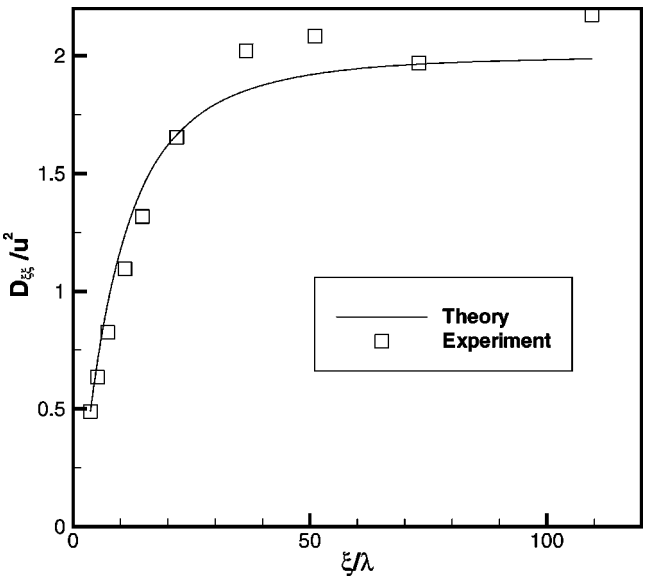

FIG. 7. Normalized second order longitudinal velocity structure function vs normalized separation, Eq. (5.29). Experiment, Tabeling *et al.* (Ref. 17).

$$\begin{aligned}\hat{D}_{\gamma\gamma,<}&=\pi U^2 na_0^3\left[4\left(\frac{\xi}{a_0}\right)^2u-\frac{125}{48}\left(\frac{\xi}{a_0}\right)^3+\frac{35}{128}\left(\frac{\xi}{a_0}\right)^5u^{-2}-\frac{27}{1792}\left(\frac{\xi}{a_0}\right)^7u^{-4}\right],\\ \hat{D}_{\gamma\gamma,>}&=\pi U^2 na_0^3\frac{40}{21}\left[u^3+\frac{2}{3}\left(\frac{a_0}{\xi}\right)^3u^6\right].\end{aligned} \tag{5.28}$$

The average over vortex size is therefore given by

$$\overline{D_{ii}}^a\left(\frac{\xi}{a_0},na_0^3,U^2,\sigma\right)=\int_0^\infty\zeta(u,\sigma)\left[\hat{D}_{ii,<}H\left(u-\frac{\xi}{2a_0}\right)+\hat{D}_{ii,>}H\left(\frac{\xi}{2a_0}-u\right)\right]du. \tag{5.29}$$

Evaluation of the above integral is carried out numerically owing to the complexity of the kernel, $\zeta(u,\sigma)$. When $\overline{D_{ii}}^a$ is nondimensionalized by the mean-square velocity, the parameters na_0^3 and U^2 cancel, leaving σ as the only remaining parameter. The value of σ is fixed by comparing the theoretical results to experiment. We utilize data for $D_{\xi\xi}$, $D_{\xi\xi\xi\xi}$, and $D_{\xi\xi\xi\xi\xi\xi}$ vs ξ/λ, where λ is the measured Taylor microscale, from the low temperature helium gas experiments of Tabeling *et al.*[17] To compare the spherical vortex model with experiment, the type-averaged Taylor microscale must first be computed so that the ratio of λ/a_0 can be obtained and used to rescale the theoretical predictions which are given as functions of ξ/a_0. Upon fixing σ, and averaging over vortex size, we obtain the Taylor microscale and the integral length scale in terms of a_0. A satisfactory fit between theory and data for $D_{\xi\xi}$ occurs when $\sigma=0.85$. Results for $D_{\xi\xi}$ and $D_{\gamma\gamma}$ are plotted in Figs. 7 and 8, respectively. The apparent nonmonotonic behavior of the data in Figs. 7, 9, and 12 is due to experimental uncertainty. The type-averaged Taylor and integral scales become

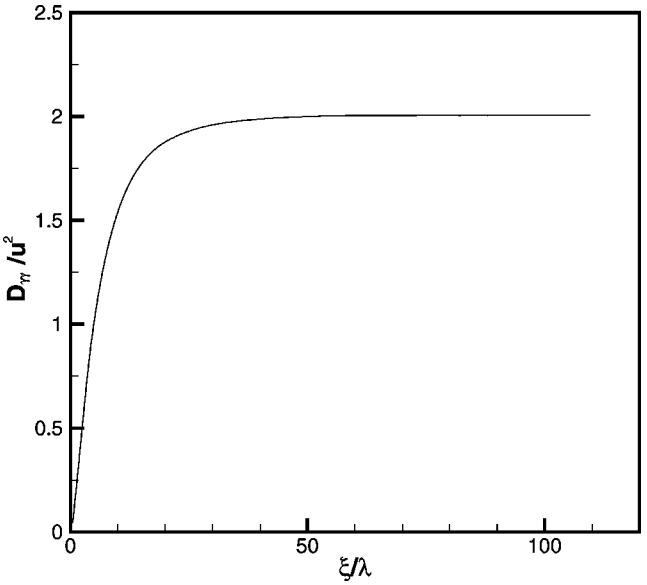

FIG. 8. Normalized second order transverse velocity structure function vs normalized separation, Eq. (5.29).

$$\overline{\lambda^a}=\sqrt{\frac{10}{21}}a_0\int_0^\infty \zeta(u,0.85)u\,du\simeq 0.99a_0, \tag{5.30}$$

$$\overline{L^a}=\frac{35}{64}a_0\int_0^\infty \zeta(u,0.85)u\,du\simeq 1.57a_0. \tag{5.31}$$

We nondimensionalize the pth order structure function by the mean square velocity (5.15). Averaging over the vortex size,

$$\overline{u^{2a}}=\frac{20}{21}\pi U^2 n a_0^3\int_0^\infty \zeta(u,0.85)u^3du\simeq 24.6 n a_0^3\pi U^2. \tag{5.32}$$

Hence, the nondimensional form for the structure function of arbitrary order is given by

$$\frac{\overline{\underbrace{D_{ij\cdots s}}^{a}}}{\langle u^2\rangle^{p/2}}=C(na_0^3)^{1-p/2}fn\left(\frac{\xi}{a_0}\right). \tag{5.33}$$

C. Results for D_{ijkl} and $D_{\xi\xi\xi\xi\xi\xi}$

The second order velocity structure function is related directly to the spectrum tensor $\Phi_{ij}(k)$. The next higher order quantity is the third order velocity structure function which, when normalized by the second order structure function, measures the skewness S, of the probability distribution of Δu_ξ. In a symmetric distribution, every odd order moment about the mean vanishes. The third order structure function plays an important role in the statistical theory of turbulence and is known generally to be nonzero by the Kármán–Howarth equation. As mentioned earlier, all odd order moments for the spherical vortex model vanish due to its high degree of symmetry. While the Kármán–Howarth equation is not violated, the vanishing of odd-order moments remains a flaw in the Hill's spherical vortex model of isotropic turbulence.

The fourth order velocity structure function tensor for isotropic turbulence is defined by (2.9). In our preferred coordinate system, the fourth order tensor D_{ijkl} is fully defined by the three independent functions $D_{\xi\xi\xi\xi}$, $D_{\gamma\gamma\gamma\gamma}$, and $D_{\xi\xi\gamma\gamma}$. Respectively these are the longitudinal, transverse and mixed structure functions defined by (4.21) and (4.22). Imposing isotropy and homogeneity on $\mu(l_i)$ and $\sigma(x_i)$ and introducing results for $D_{\xi\xi}$ and $D_{\gamma\gamma}$, these equations become

$$D_{iiii}=\frac{n}{4\pi}\int d\mathbf{x}\int d\mathbf{\Omega}(\tilde{u}_i-u_i)^4+3D_{ii}^2, \tag{5.34}$$

where $i=\xi$ or γ, and

$$D_{\xi\xi\gamma\gamma}=\frac{n}{4\pi}\int d\mathbf{x}\int d\mathbf{\Omega}(\tilde{u}_\xi-u_\xi)^2(\tilde{u}_\gamma-u_\gamma)^2+D_{\xi\xi}D_{\gamma\gamma}. \tag{5.35}$$

Analytical evaluation of these integrals is carried out in the same manner as those involved in the calculation of D_{ij}. Two cases are considered separately and the domain of integration is partitioned appropriately. Upon introducing the transformation to toroidal coordinates, the integrands involve terms like $r^\alpha\tilde{r}^\beta\tau(\varphi)$, where $\tau(\varphi)$ is a trigonometric function. The large number of such terms involved and the complicated limits of integration render the problem intractable without the aid of technical computing software.

To average the fourth order statistics over vortex size, we make the substitution $\varphi=\psi\mathcal{L}/u$, where $\psi=\xi/\overline{\lambda^a}$, $\mathcal{L}=\overline{\lambda^a}/a_0$, and $u=a/a_0$. The type averaged integrals for $D_{\xi\xi\xi\xi}$, $D_{\gamma\gamma\gamma\gamma}$, and $D_{\xi\xi\gamma\gamma}$ are given as follows:

$$\begin{aligned}\overline{D_{\xi\xi\xi\xi}}^a(\psi,na_0^3)=na_0^3\pi U^4\int_0^\infty\zeta(u,\sigma=0.85)\Bigg[&\hat{D}_{\xi\xi\xi\xi,>}\\&\times H\left(u-\frac{\varphi}{2}\right)+\hat{D}_{\xi\xi\xi\xi,>}H\left(\frac{\varphi}{2}-u\right)\Bigg]du\\&+3\Bigg\{\int_0^\infty\zeta(u,\sigma=0.85)\Bigg[\hat{D}_{\xi\xi,<}H\left(u-\frac{\varphi}{2}\right)\\&+\hat{D}_{\xi\xi,>}H\left(\frac{\varphi}{2}-u\right)\Bigg]du\Bigg\}^2,\end{aligned} \tag{5.36}$$

$$\begin{aligned}\overline{D_{\gamma\gamma\gamma\gamma}}^a(\psi)=na_0^3\pi U^4\int_0^\infty\zeta(u,\sigma=0.85)\Bigg[&\hat{D}_{\gamma\gamma\gamma\gamma,<}H\left(u-\frac{\varphi}{2}\right)\\&+\hat{D}_{\gamma\gamma\gamma\gamma,>}H\left(\frac{\varphi}{2}-u\right)\Bigg]du\\&+3\Bigg\{\int_0^\infty\zeta(u,\sigma=0.85)\Bigg[\hat{D}_{\gamma\gamma,<}H\left(u-\frac{\varphi}{2}\right)\\&+\hat{D}_{\gamma\gamma,>}H\left(\frac{\varphi}{2}-u\right)\Bigg]du\Bigg\}^2,\end{aligned} \tag{5.37}$$

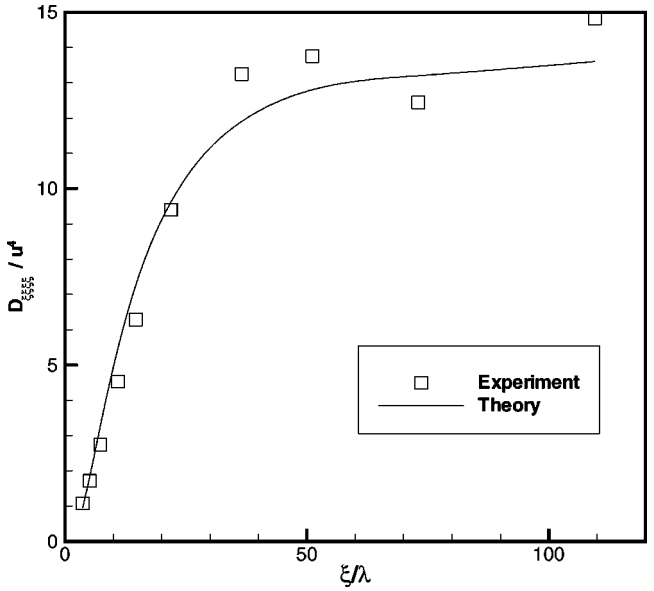

FIG. 9. Fourth order normalized longitudinal velocity structure function vs normalized separation, Eq. (5.36). Experiment, Tabeling *et al.* (Ref. 17).

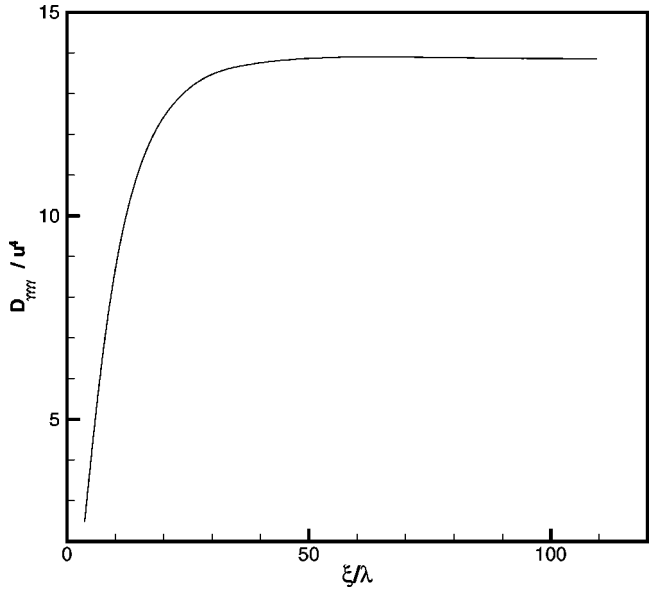

FIG. 10. Fourth order normalized transverse velocity structure function vs normalized separation, Eq. (5.37).

$$\overline{D_{\xi\xi\gamma\gamma}}^a(\psi)=na_0^3\pi U^4\int_0^\infty \zeta(u,\sigma=0.85)\left[\hat{D}_{\xi\xi\gamma\gamma,<}H\left(u-\frac{\varphi}{2}\right)+\hat{D}_{\xi\xi\gamma\gamma,>}H\left(\frac{\varphi}{2}-u\right)\right]du+\left\{\int_0^\infty \zeta(u,\sigma=0.85)\times\left[\hat{D}_{\xi\xi,<}H\left(u-\frac{\varphi}{2}\right)+\hat{D}_{\xi\xi,>}H\left(\frac{\varphi}{2}-u\right)\right]du\right\}\times\left\{\int_0^\infty \zeta(u,\sigma=0.85)\left[\hat{D}_{\gamma\gamma,<}H\left(u-\frac{\varphi}{2}\right)+\hat{D}_{\gamma\gamma,>}H\left(\frac{\varphi}{2}-u\right)\right]du\right\}. \tag{5.38}$$

Upon nondimensionalizing by the root-mean-square velocity raised to the order of the statistic, the nth order structure function contains the quantity $(na_0^3)^{1-n/2}$. This term is unity for $n=2$, allowing us to tune the variance σ in the size distribution so that satisfactory agreement with experimental data can be achieved. We choose to fix the remaining parameter na_0^3 by fitting the fourth order longitudinal prediction to experimental data.[17] A satisfactory fit between the statistical model and experiment occurs when $na_0^3=0.020$. Quadrature results for (5.36), (5.37), and (5.38) are provided in Figs. 9, 10, and 11. When these parameter values are set, the lateral and mixed results are predictions.

We now have a parameter free statistical model for homogeneous isotropic turbulence and wish to make a prediction for the sixth order longitudinal velocity structure function, $D_{\xi\xi\xi\xi\xi\xi}$. For N statistically independent vortices, this is defined by (4.23). Imposing isotropy and homogeneity in the usual way, we find

$$D_{\xi\xi\xi\xi\xi\xi}=\frac{n}{4\pi}\int d\mathbf{x}\int d\mathbf{\Omega}(\tilde{u}_i-u_i)^6+15D_{\xi\xi}D_{\xi\xi\xi\xi}. \tag{5.39}$$

Type-averaged results for (5.39) are given in Fig. 12. We see that Hill's spherical vortex coupled with details on the probability distribution of $(\tilde{u}_i-u_i)$ produce a turbulence model consistent with experimental velocity structure function data orders 2, 4, and 6.

VI. CONCLUDING REMARKS

Synge and Lin obtained theoretical second order velocity correlation curves for a Hill's spherical vortex model of isotropic turbulence, which demonstrated fair agreement with experiment. We have extended their statistical analysis beyond the second order and have introduced a new model feature consisting of log-normal statistics for the vortex radii. A mathematical model for computing the ensemble average

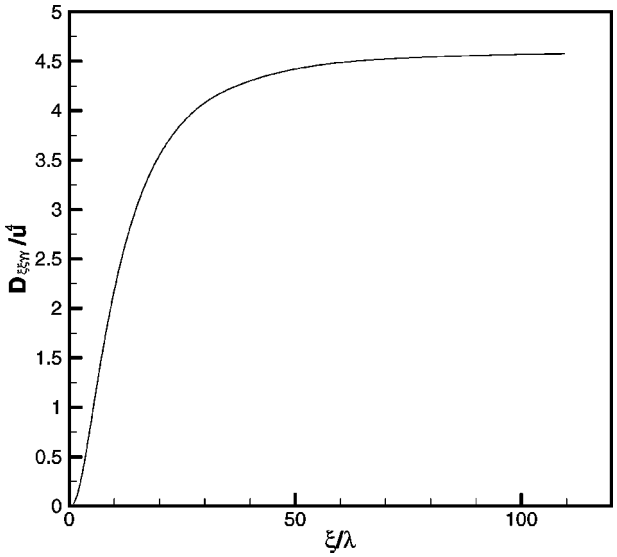

FIG. 11. Fourth order mixed structure function vs normalized separation, Eq. (5.38).

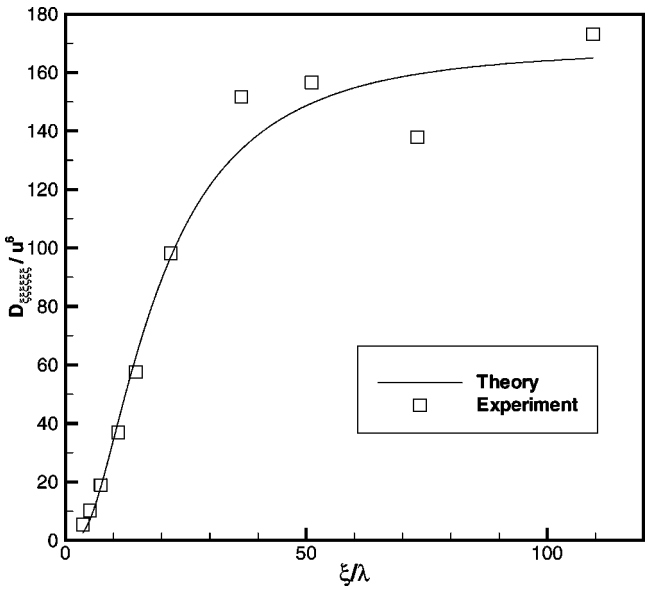

FIG. 12. Sixth order longitudinal velocity structure function. Experiment, Tabeling *et al.* (Ref. 17).

was derived and used to obtain complete velocity structure function information for orders two and four, and the longitudinal component of the sixth order tensor. The model was developed around the longitudinal second and fourth order velocity structure functions. Two free parameters were determined such that these statistics gave fair agreement with empirical data for high Reynolds number isotropic flows. The second order lateral structure function was derived independently of $D_{\xi\xi}$ as verification of the longitudinal results. The model was then used to predict the higher order velocity statistics, the fourth order lateral, fourth order mixed, and the sixth order longitudinal structure functions, $D_{\gamma\gamma\gamma\gamma}$, $D_{\gamma\gamma\xi\xi}$, and $D_{\xi\xi\xi\xi\xi\xi}$, respectively. At large Reynolds numbers, we found good agreement between experiment and the sixth order longitudinal prediction. This is the main result of the present paper. Our predictions for the lateral and mixed fourth order can be compared with data as these become available. The model can, in principal, be used to calculate velocity structure functions of any order.

While the model appears robust in its predictive capability, it is not without inconsistencies. Foremost, the high degree of symmetry causes all odd-order structure functions to vanish which is contrary to theory, experiment and simulation. One suggestion for breaking the symmetry is to add helicity to the flow.[23] While this would probably be a more physically viable model, the analytical tractability would be quickly lost. Furthermore, the spherical vortex is not a perfect model for a turbulent eddy. The velocity field is continuous across the vortex surface, but there is a discontinuity in the tangential rate of shear. In a viscous fluid this discontinuity would become dynamically significant and would quickly alter the motion. A model better suited to understanding the general decay of turbulence would not contain such a defect and would include some type of viscous dissipation mechanism. One such approach would be to seek a viscous perturbation of Hill's spherical vortex by introducing a small amount of viscosity on the vortex surface.

ACKNOWLEDGMENTS

The authors acknowledge many useful discussions with Philip Saffman. We also thank Patrick Tabeling for supplying detailed measurements of longitudinal velocity structure functions.

[1] J. L. Synge and C. C. Lin, ''On a statistical model of isotropic turbulence,'' Trans. R. Soc. Can. **37**, 45 (1943).
[2] A. A. Townsend, ''On the fine scale structure of turbulence,'' Proc. R. Soc. London, Ser. A **208**, 534 (1951).
[3] S. Corrsin, ''Turbulent dissipation fluctuations,'' Phys. Fluids **5**, 1301 (1962).
[4] A. A. Tennekes, ''Simple model for the small-scale structure of turbulence,'' Phys. Fluids **11**, 669 (1968).
[5] P. G. Saffman, ''Lectures on homogeneous turbulence,'' in *Topics in Nonlinear Physics*, edited by N. J. Zabusky (Springer-Verlag, Berlin, 1968).
[6] T. S. Lundgren, ''Strained spiral vortex model for turbulent fine structure,'' Phys. Fluids **25**, 2193 (1982).
[7] D. Segel, ''The higher moments in the Lundgren model conform with Kolmogorov scaling,'' Phys. Fluids **7**, 3072 (1995).
[8] D. I. Pullin and P. G. Saffman, ''On the Lundgren–Townsend model of turbulent fine scales,'' Phys. Fluids A **5**, 126 (1993).
[9] D. I. Pullin, J. D. Buntine, and P. G. Saffman, ''On the spectrum of a stretched spiral vortex,'' Phys. Fluids **6**, 3010 (1994).
[10] D. I. Pullin and P. G. Saffman, ''Vortex dynamics in turbulence,'' Annu. Rev. Fluid Mech. **30**, 31 (1998).
[11] D. I. Pullin, ''Pressure spectra for vortex models of homogeneous turbulence,'' Phys. Fluids **7**, 849 (1995).
[12] T. S. Lundgren, ''The concentration spectrum of the product of a fast biomolecular reaction,'' Chem. Eng. Sci. **40**, 1641 (1985).
[13] A. Roshko, ''Experiments on the flow past a circular cylinder at very high Reynolds number,'' J. Fluid Mech. **10**, 345 (1961).
[14] Y. T. Couder O. Cadot, and S. Douady, ''Characterization of the low-pressure filaments in a three-dimensional turbulent shear flow,'' Phys. Fluids **7**, 630 (1995).
[15] M. Farge, N. Kevlahan, V. Perrier, and E. Goirand, ''Wavelets in turbulence,'' Proc. IEEE **84**, 639 (1996).
[16] A. N. Kolmogorov, ''A refinement of previous hypotheses concerning the local structure of turbulence in a viscous incompressible fluid at high Reynolds number,'' J. Fluid Mech. **12**, 82 (1962).
[17] P. Tabeling, G. Zocchi, F. Belin, J. Maurer, and H. Willaime, ''Probability density functions, skewness, and flatness in large Reynolds number turbulence,'' Phys. Rev. E **53**, 1613 (1996).
[18] A. S. Monin and A. M. Yaglom, *Statistical Fluid Mechanics: Mechanics of Turbulence* (MIT Press, Cambridge, 1975).
[19] M. J. M. Hill, ''On a spherical vortex,'' Philos. Trans. R. Soc. London **185**, 213 (1894).
[20] H. P. Robertson, ''The invariant theory of isotropic turbulence,'' Proc. Cambridge Philos. Soc. **36**, 209 (1940).
[21] A. M. Yaglom, ''Lagrangian turbulence characteristics in a diabatic atmospheric surface layer and in convective jets,'' Izv. Akad. Nauk SSSR, Ser. Fiz. **1**, 157 (1965).
[22] L. P. Bernal, ''The statistics of the organized vortical structure in turbulent mixing layers,'' Phys. Fluids **31**, 2533 (1988).
[23] P. G. Saffman, *Vortex Dynamics* (Cambridge University Press, Cambridge, 1992).